Kent Academic Repository

Full text document (pdf)

Citation for published version

Zhou, Y. and Zhu, F. and Gao, Steven and Luo, Qi and Wen, L. and Wang, Q. and Yang, X.X. and Geng, Y.L. and Cheng, Z.Q. (2018) Tightly Coupled Array Antennas for Ultra-Wideband Wireless Systems. IEEE Access . ISSN 2169-3536.

DOI

https://doi.org/10.1109/ACCESS.2018.2873741

Link to record in KAR

https://kar.kent.ac.uk/69265/

Document Version

Publisher pdf

Tightly Coupled Array Antennas for Ultra-Wideband Wireless Systems

Y. Zhou[1], (Member, IEEE), F. Zhu[2], S. Gao[3], (Senior Member, IEEE), Q. Luo[3], L. Wen[3], Q. Wang[3], X.X. Yang[4], Y.L. Geng[5] and Z.Q. Cheng[5]

[1]College of electronic and information engineering, Nanjing University of Aeronautics and Astronautics, Nanjing 211106, China
[2]Science and Technology on Antenna and Microwave Laboratory, Nanjing 210039, China
[3]School of Engineering and Digital Arts, University of Kent, Canterbury, UK
[4]Key Lab of Specialty Fiber Optics and Optical Access Networks, Shanghai University, Shanghai, China
[5]School of Electronic Engineering, Hangzhou Dianzi University, Hangzhou, China

Corresponding author: Yonggang Zhou (zyg405@nuaa.edu.cn)

ABSTRACT Tightly coupled array (TCA) antenna has become a hot topic of research recently, due to its potential of enabling one single antenna array to operate over an extremely wide frequency range. Such an array antenna is promising for applications in numerous wideband/multi-band and multi-function wireless systems such as wideband high-resolution radars, 5G mobile communications, satellite communications, global navigation satellite systems, sensors, wireless power transmission, internet of things and so on. Many papers on this topic have been published by researchers internationally. This paper provides a detailed review of the recent development on TCA that utilizes the capacitive coupling. The basic principles and the historical evolution of the TCAs are introduced firstly. Then, recent development in the analysis and design of TCAs, such as equivalent circuit analysis, bandwidth limitation analysis, array elements, feed structures, substrates/superstrates loading, etc., are explained and discussed. The performances of the state-of-the-art TCAs are presented and a comparison amongst some TCAs reported recently is summarized and discussed. To illustrate the practical designs of TCA, one case study is provided, and the detailed design procedures of the TCA are explained so as to demonstrate the TCA design methodology. Simulated results including the VSWR at different angles of scanning, patterns and antenna gain are shown and discussed. A conclusion and future work are given in the end.

INDEX TERMS Antennas, Tightly coupled arrays, Ultra wideband antennas, Antenna arrays, Ultra-wideband systems

I.INTRODUCTION

With the development of numerous wireless systems such as wideband high-resolution radar, high-throughput mobile and satellite communication, global navigation satellite systems, wireless power transmission, electronic warfare, software-defined radio, ultra-wideband (UWB) array antennas that have a compact size and can operate over a wide range of frequencies have attracted significant interests due to their potential of realizing multiple functions within one single radiating aperture. These multiple functions are usually achieved by using many separate antenna arrays operating at different frequency bands; hence a significant reduction of the size, weight, cost and power consumption of wireless systems can be achieved by using UWB array antennas.

In addition to the bandwidth requirement, antennas used in practical UWB and multifunction systems usually need to meet other requirements, such as low profile, wide-angular-range beam steering, high polarization purity and high isolation between different polarization ports, etc. It is a challenge to design a single UWB radiating aperture that fulfills all the requirements.

Recently, a new class of antenna array referred to as tightly coupled arrays (TCAs), has been demonstrated to be able to achieve UWB performance. Up to date, many papers have been published on this topic. There are two main types of TCAs, one is based on the use of the connected arrays and the other is based on the capacitively coupling. This article will mainly focus on the TCAs using the capacitive coupling because it can better demonstrate the principle of increasing bandwidth by using coupling capacitance to counteract the ground plane inductance. This paper aims to provide a detailed review of the recent development on TCA that utilizes the capacitive coupling. The basic principles and the historical evolution of the TCAs are introduced, and this is then followed by a review of recent development in the analysis and design of TCAs, such as equivalent circuit analysis, bandwidth limitation analysis, array elements, feed structures, substrates/superstrates loading, etc. The performances of the state-of-the-art TCAs are provided and some recent TCAs reported are compared, summarized and discussed. To illustrate the detailed design of TCA, one case study is also provided, showing the step-by-step design considerations of the TCA. Many simulated results including the VSWR at different angles of scanning, patterns and antenna gain are presented and explained. Finally, a conclusion and future work in TCAs are given.

II. THE BASIC PRINCIPLES AND HISTORY OF THE TCA

A. BASIC CONCEPTS OF THE TCA

Usually, antenna array design starts with designing an isolated element that has the desired bandwidth and radiation characteristics and then reducing the mutual coupling effect between array elements. Various methods have been proposed to mitigate undesired coupling between elements, such as adding cavities behind each element, introducing conductive traces or wave absorber around elements. The design of broadband phased arrays with large scan volume is even more challenging due to the small element separation. In order to avoid grating lobes, an array lattice of one-half wavelength of the highest operating frequency is usually required when the main beam needs to be scanned in large volume, thus resulting in the small element spacing and strong mutual coupling at the lowest working frequency. The inherent strong mutual coupling in lower frequency band limits the performances of UWB phased arrays.

Recently, a novel class of arrays referred to as TCA was proposed. The operating principle of the TCA is fundamentally different from that of the traditional antenna array. In TCA, very small elements (compared with the lowest operating wavelength) are spaced very close to each other and strong mutual coupling between them is intentionally introduced. In this way, the array can support current with a wavelength much larger than the size of the element, thus the low-frequency end of the TCA can be

significantly extended while the high-frequency limit which is determined by the onset of grating lobs remains nearly unaffected. In addition, the TCA usually has some desirable properties such as low profile, large grating-lobe free scan volume and high polarization isolation.

B. DEVELOPMENT HISTORY

The concept of the TCA, which places electrically small elements very close to each other, was originated from Wheeler's current sheet antenna (CSA) [1]. The coupling capacitance between the elements was used to keep the current continuous, and the ideal infinite continuous CSA without ground had stable input impedance, which implied that an antenna can have an unlimited bandwidth. However, planar arrays are normally required to have a ground plane for directional radiation. At the lower frequency, the distance from the ground plane to the arrays is electrically small; the ground plane will short-circuit the array and result in inefficient radiation. Because of this, the CSA with the ground plane no longer has an unlimited bandwidth. In terms of current continuity, the TCA is a type of connected array. In this paper, we focus on capacitive tightly coupled arrays. Zero impedance connected arrays and long slot arrays in which radiation elements are connected directly fall out of the scope of this paper.

In 2003, Ben Munk from the Ohio State University demonstrated a tightly coupled dipole array (TCDA) which was the first practical implementation of Wheeler's theoretical "current sheet" concept with a ground plane below the radiating aperture [2]. Some of that work was based on the author's extensive experience in the field of frequency selective surface (FSS) [3]. The coupling capacitor was not only used to make the current continuous but also to counteract the ground plane inductance, thereby increasing the antenna bandwidth. In collaboration with Harris Corporation, aforementioned TCDA with a bandwidth of 9:1 was designed and measured [4]. Several methods including placing dielectric superstrate, magnetic or lossy substrate above the ground plane were suggested by Munk for further increasing the bandwidth of the TCDA.

Having the TCDA as a benchmark, a series of TCAs have been published by the research group of the Ohio State University since 2009. Various elements, feed structures, loading superstrates/substrates and coupling structures were developed. The array performance, such as bandwidth, scan volume, etc., were greatly improved [5-7, 11-14, and 16-21]. At the same period, some fundamental research works such as equivalent circuit extraction, bandwidth limit analysis were also carried out [8, 9, 10, and 15].

Based on the same methodology, the Virginia Polytechnic Institute and State University antenna group proposed tightly coupled foursquare arrays [25，26]. These arrays were based on broad-band crossed-dipole type antenna radiating elements [27] and could achieve circular polarization. Contemporaneously, Planar Ultra-wideband Modular

Antenna (PUMA) arrays which can be regarded as low-cost, wide-scan, and low-cross dual polarized TCAs were developed [28-31]. The PUMA arrays were designed to simplify the feed structure while also remaining good broadband and scan performances.

In 2011, supported by "The Square Kilometre Array" project, TCAs using octagonal ring elements were published and continuously improved [32-35]. After 2015, increasing number of research groups contributed to the TCAs area and more and more papers were published. The research topics include equivalent circuits [36, 37], bandwidth limit [38], elements [39-43], feed structures (BALUNs and matching networks) [44-49], superstrate/substrate [50-55], system application [22, 23, 24, and 56-59], etc. Those TCAs' research topics will be presented in detail in the next section.

Ⅲ. RECENT DEVELOPMENT in TCA

A. EQUIVALENT CIRCUIT ANALYSIS

In antenna arrays design, the equivalent circuit method is an extremely powerful tool. It can be used to illustrate the physical phenomena and guide the antenna arrays design. B.Munk proposed a simplified equivalent circuit for TCDA backed by a ground plane. It can well explain the principle that the low-frequency end of the TCDA above a ground plane can be extended. The equivalent circuit was obtained by analyzing infinite array without considering the edge effect of the finite array.

For one element in an infinite TCDA, the ground plane can be regarded as a short-circuited transmission line in parallel with the input impedance of dipole, as shown in Fig. 1. In the low frequencies, the distance from the ground to the dipole is usually less than 1/4 wavelength and the reactance from the ground is inductance. The radiation resistance becomes very small, near zero, because the paralleled ground inductance is proportional to the frequency. To compensate for the ground inductance, the coupling capacitance between neighboring elements is introduced and the low-frequency limit is extended. It is worth pointing out that the equivalent circuit is only a simplified circuit model, which can be used to explain the physics of the problem and cannot be used for obtaining actual calculated values.
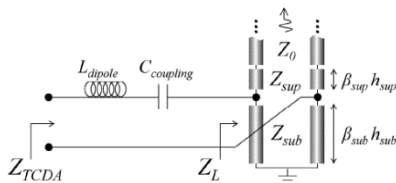

FIGURE 1. Munk's equivalent circuit [13]

Based on Munk's equivalent circuit model, the equivalent circuit of the tightly coupled spiral array with interwoven arm spirals was proposed in [9], as shown in Fig. 2. The equivalent circuit consisted of transmission lines (TLs) and a combination of lumped elements. It also included the higher-

order modes supported by the transmission lines. In the proposed equivalent circuit, the spiral was modeled by cascade of TL sections and the interwoven arms as two TLs in series terminated by lumped elements. The proposed equivalent circuit was used to optimize the superstrate permittivity and thickness of a TCA with the spiral element and a VSWR<3 impedance bandwidth of 20:1was achieved.
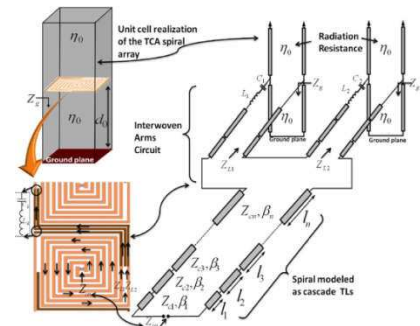

FIGURE 2. The equivalent circuit for spiral array [9]

In [36], the authors proposed an improved ultra-wideband equivalent circuit model for connected TCDA as well as capacitance coupled TCDA, which was more accurate over a wide frequency band than Munk's model, and it modeled the array input impedance in both broadside and scan configurations, as shown in Fig. 3. In Fig. 3, similar to Munk's model, L_1 was the dipole's self-inductance and C_1 was the coupling capacitor; Z_0 denoted the radiation resistance of the array located in a semi-infinite space; capacitance C_2 and inductance L_2 were the components added to Munk's model. A set of equations were given to determine the values of the components in Fig. 3 (see the equations (1)-(3) in [36]). The input impedance of an example array was calculated using Munk's model, the new equivalent circuit, and a full-wave simulation respectively were given in [36]. The results obtained by the new equivalent circuit agreed well with the results obtained by full-wave analysis over the operating frequency band from DC to the first free-space grating lobe frequency, thus the accuracy of the new equivalent circuit was proved. Based on the equivalent circuit model, a TCDA with multilayer superstrates was optimized to achieve the best performances in both bandwidth and scanning capability.
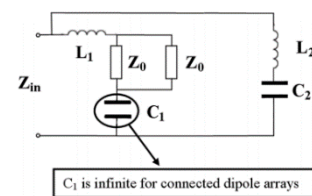

FIGURE 3. Equivalent circuit in [36]

Aforementioned equivalent circuits model one element in infinite arrays. Green's function based equivalent transmission line model for the analysis of finite TCAs and connect arrays was developed in [37] to describe the

propagation of the edge-born guided waves along the finite array, as shown in Fig. 4. Active impedances of array elements were represented as periodic loads on the equivalent transmission line. The equivalent model can be used to preliminary and fast estimate the performance of finite arrays and minimize the edge effects.
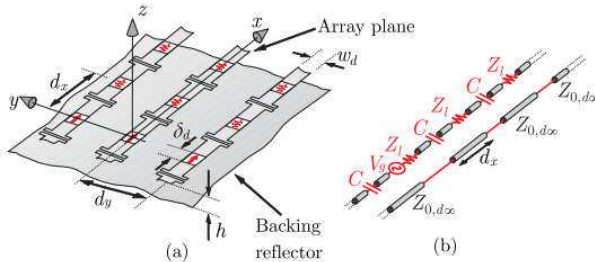

FIGURE 4. (a) Array of tightly coupled dipoles with ground plane excited at one edge. (b) Equivalent transmission line [37].

B. BANDWIDTH LIMITS ANALYSIS

As mentioned above, in theory, Wheeler's CSA is frequency independent. However, usually, the planar array has a ground plane, and then the bandwidth of the planar array is no longer infinite. Estimating the theoretical bandwidth limit of arrays has important significance in guiding the design of broadband antenna arrays. The research team from the Ohio State University has done a series of works on this topic [8, 10, and 15]. In [8], a simple equivalent circuit model similar to Munk's one, as shown in Fig 5, was developed to derivate the theoretical limit that held for any lossless planar array above a ground plane. By applying Fano's impedance matching approach and Richard's transformation, maximum bandwidth limits, which were functions of impedance mismatch, substrate & superstrate parameters and aperture complexity, were given.
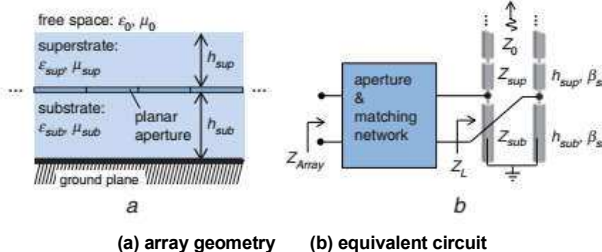

(a) array geometry   (b) equivalent circuit
FIGURE 5. Equivalent circuits of the planar array above ground plane used to analyze bandwidth limit [8]

In [10], the same research group extended the study of bandwidth limit developed in [8] to including the dependence on height and scan angle of PEC-backed planar arrays. A simple expression for the maximum bandwidth of the low-profile scanning array under the TE or TM excitation was given by equations (28) & (29) in [10]. Based on the work in [10], the authors further extended the limits to considering simultaneous excitation of both TE and TM modes [15]. A more general bandwidth limit for lossless and reciprocal PEC-backed planar arrays (LRPBA) was developed. Maximum impedance bandwidth for a linearly polarized LRPBA was given by the equation (44) in [15], and for a circularly polarized LRPBA, the larger impedance bandwidth can be obtained by sacrificing the polarization purity. Similarly, based on [15], the higher-order Fano-type bandwidth limit was derived using the plane-wave scattering analysis [38]. Unlike the limits given in [15], higher-order impedance bandwidth limits were deduced in terms of the scan angles, the array thickness as well as the element characteristics such as the element polarizability, unit cell dimensions, and so on.

C. ELEMENT AND COUPLING

Traditionally, to design wideband arrays, wideband antenna elements which can work in the entire operating band are adopted. Instead of using elements with a sufficient working bandwidth, the TCAs employ coupled electrically small elements which do not have to be broadband. However, broadband antenna elements with simple structure are preferred. The basic types of elements widely used in planar ultrawide bandwidth TCAs are spirals, patches and dipoles. Long slot antenna arrays are considered to be connected arrays, which will not be discussed in this paper. Tapered slot or Vivaldi elements have a bandwidth of more than 10:1; however, their thickness is too large to be considered as low-profile. Meanwhile, so-called tightly coupled Vivaldi arrays usually refer to arrays with directly connected Vivaldi elements, which will not be demonstrated here.

1) SPIRAL ELEMENT

Interconnected Self-complementary structures such as bowtie and spiral arrays exhibit good radiation performances at low frequency in free space. However, its radiation performance deteriorates when placed above a ground plane, which is caused by the highly paralleled inductive admittance. Interconnected spiral array exhibits much more stable real and imaginary impedances across the operating bandwidth than the connected dipole type array. Concurrently, the low-frequency performance can be substantially improved by introducing the coupling capacitance between the elements to counteract the ground inductance. In [5], an interwoven structure in which the elements have their arms "interwoven" to enhance coupling was proposed, and a 10:1 impedance bandwidth (VSWR<2) was achieved without the use of dielectric superstrates or lossy materials. The unit cell was only $\lambda_h/1.83 \times \lambda_h/1.83$ and placed $\lambda_h/1.83$ above the ground plane, here λ_h is the wavelength of the highest frequency, as shown in Fig. 6. What needs to be explained is that the reported performance is based on an infinitely array for broadside scan and a poor polarization isolation of only 7dB is observed in the operating band.
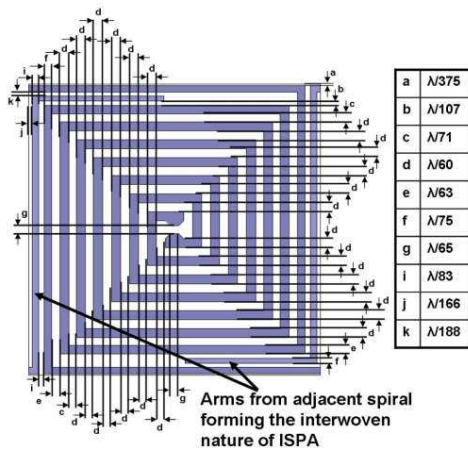
FIGURE 6. Interwoven spiral array unit cell and its dimensions in wavelengths [5]

2) DIPOLE TYPE ELEMENT

Most of the elements for planar TCAs have geometries derived from the dipole. Although they have different shapes, their fundamental properties are the same. They are balanced structures with a resonant length of $\lambda/2$ when isolated. The bandwidth of an isolated dipole is not wide, even methods of broadening bandwidth are applied, the typical bandwidth ranges between 10%-30%, but much wider bandwidth is possible for the TCDAs. The element of the TCDA usually has a size of about $\lambda/2$ at the highest operating frequency and is placed above a ground plane with an approximate distance of $\lambda/4$ at the center frequency. The shape and arrangement of elements which determine the self-inductor and coupling capacitor of elements can be optimized by the aforementioned equivalent circuit models. The unit shapes and arrangements are different in various TCDAs.

Ben Munk and Harris Corporation's TCDAs presented in [2, 4], which are the first practical implementations of Wheeler's "current sheet" concept, adopted simple dipoles as elements. Interdigital capacitors between elements were introduced to implement the inter-element coupling. The TCA in [2] has a bandwidth around 4:1 with a VSRW<2:1, and the bandwidth can be further extended to 7:1 by loading multi-layer thin dielectric superstrate. A dual-polarization TCDA designed for 2-18GHz and a VHF/UHF TCDA breadboard were demonstrated in [4]. For the 2-18GHz sample, a bandwidth of approximately 9:1 (VSWR<3:1) was obtained. The VHF/UHF TCDA, removed from the cavity in order to show detail, is shown in Fig. 7.

FIGURE 7. TCDA breadboard for VHF/UHF band [4]

Having the aforementioned TCDA as a benchmark, the Ohio State University group developed a series of TCAs, which usually used dipoles as the elements. In [13], dipole elements were printed on vertical boards in order to integrate with compact Marchand baluns, as shown in Fig. 8. The dipole's self-inductance was controlled by the height of dipole, and the coupling capacitance was created by the overlap of the dipole arms which were printed on the opposite faces of a PCB. The designed TCA in [13] had a bandwidth of 7.35:1(VSWR<2.65:1) while scanning to $\pm45^o$ in E and H planes. Similar vertical printed dipoles with overlapping coupling capacitances were used in [11, 17]. A superior performance of 6.1:1 bandwidth (0.5–3.1 GHz) with VSWR<3.2 when scanning ±75° in E plane, ±70° in D plane and ±60° in H plane was achieved in [17]. In [61], the dipole arms were printed on the same surface of a vertical board and lumped or distributed capacitors were used as coupling capacitors.
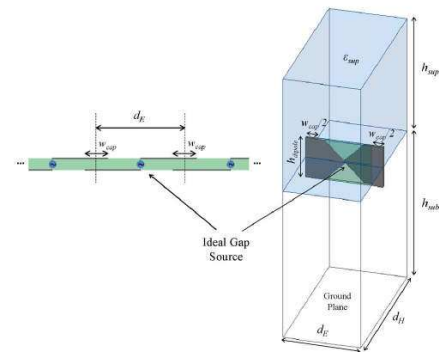
FIGURE 8. The dipole element in [13]

The advantage of the vertical printed dipole is that it is easy to integrate with the feed structure. Meanwhile, the horizontally printed radiator is also extensively employed. In [7], a low-profile TCDA employing a resistive frequency selective surface (FSS) and a superstrate was introduced. The TCDA had a bowtie unit which can be considered as a dipole type antenna, as shown in Fig. 9. The resistive FSS was used to suppress $\lambda/2$ resonant induced by ground plane, and a superstrate was adopted to mitigate resistive loss of FSS. The proposed array achieves desirable performances such as, very low profile ($0.055\lambda_l$, where λ_l represents the wavelength at the lowest working frequency), 21:1 bandwidth (broadside

This article has been accepted for publication in a future issue of this journal, but has not been fully edited. Content may change prior to final publication. Citation information: DOI
10.1109/ACCESS.2018.2873741, IEEE Access

Y. Zhou, F. Zhou, S.Gao etc.: Preparation of Papers for IEEE Access
(September 2018)

radiation, infinite array) and a radiation efficiency greater than 73% across the frequency band. Based on the similar horizontal dipole type element, the scanning and dual-polarized TCDAs were developed and reported in [14] and [21].
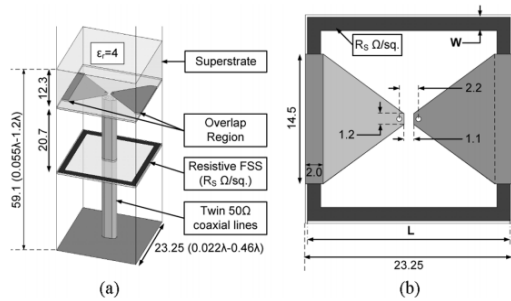

FIGURE 9. The dipole element in [7]

The TCDA in [12] had non-symmetric horizontal dipole elements, which introduced the coupling with a novel ball-and-cup structure, as shown in Fig. 10. Using the non-symmetric qualities of the unit, wideband and wide-angle scanning performances were achieved. The TCAD had a thickness of $\lambda_l/8$ at the lowest working frequency (8GHz), an active VSWR less than 2 from 8-12.5 GHz while scanning up to 70° and 60° in E- and H-plane, respectively.
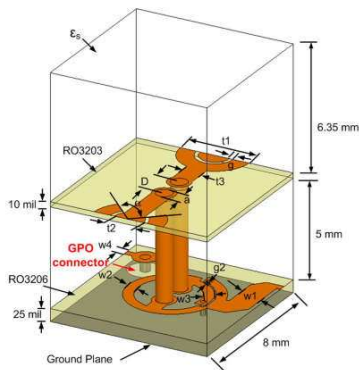

FIGURE 10. The dipole element in [12]

A whole family of TCDAs referred as planar ultra-wideband modular array (PUMA) use normal dipole elements [28-31]. Array element in [30] is demonstrated in Fig. 11. The shape and coupling principle are the same as the initial TCPA, but shorting vias were adopted to reduce the common resonant. Each of PUMA family members had novel feeding scheme that eliminated the need for complex feeding structures such as baluns, "cable organizers", etc. In addition, all PUMA arrays consist of dual-offset dual-polarized lattice arrangements for modular tile-based assembly. The PUMA in [30] exhibited a measured active VSWR < 2.8 over 7-21GHz with scanning angle up to 45° in E and H planes.
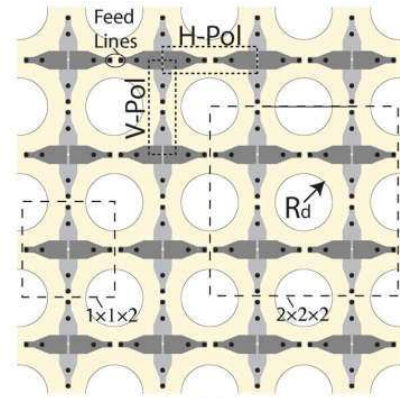
(a) Top view of PUMA
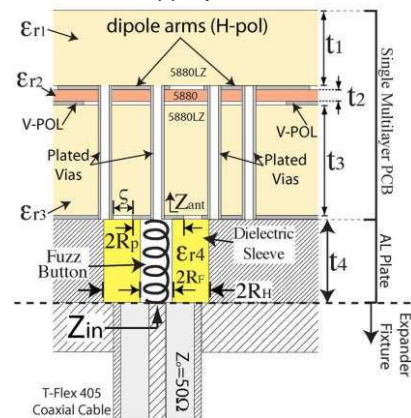
(b) Cross section of the unit cell

FIGURE 11. Dual-polarized PUMA array [30]

Highly coupled octagonal ring pairs which can be considered as variant dipoles were employed in [32-35] to develop a family of TCAs referred as octagonal ring antenna (ORA) arrays. This array was applied to the square kilometer array (SKA) project. This type of array requires bandwidth exceeding 3.3:1, a maximum scan angle of ±45° and low cost etc. The initial design in [32] is given in Fig. 12, where a shared ring was used to implement dual-polarization and a tight coupling between octagonal ring pairs was implemented with an interdigital capacitor. In [33], the octagonal ring pair in [32] evolved into a fractal octagonal ring pair.
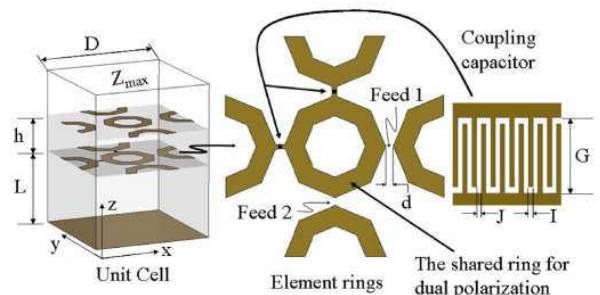

FIGURE 12. Octagonal Ring Element [32]

Foursquare element was proposed by J. R. Nealy [27], as shown in Fig. 13. One may view the foursquare element as a dipole structure. For a single polarization feed (via "a" and

"a'" feed points), the patch 12 and 18 in Fig. 13 act as dipole arms and the parasitic patch 14 and 16 serve as a sleeve. A foursquare element has properties such as small size, low-frequency response, moderately wide bandwidth and dual-polarization, and is suited to array applications. Appling the foursquare element, the Virginia Tech developed a series TCAs [25, 26], a simulated 7.24:1 (VSWR<3) bandwidth in an infinite array with high efficiency was achieved [26].
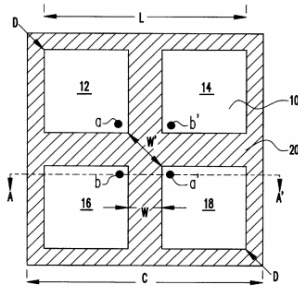

FIGURE 13. **Foursquare element [27]**

Some dipole type elements for TCDAs, which can be considered as aforementioned elements with minor modification in the shape and coupling structure, were proposed in [39-43]. These types of elements are not introduced in detail here for the purpose of conciseness.

3) PATCH ELEMENT

Although dipole type elements are intensively used in the TCA design, the dipole type element usually has a very high input impedance, which is hard to match with a typical coaxial line with a $50\,\Omega$ character impedance. Therefore, an additional balun with a function of impedance transform is needed. This additional balun undoubtedly increases the array complexity and cost. In order to avoid the additional balun, some TCAs using the patch element (tightly coupled patch arrays, TCPAs) were developed [66, 67], as shown in Fig. 14. In Fig. 14, the element can be viewed as a $L_d \times W_d$ patch on a substrate with a size of $L \times W$ and is split into two pieces with a slot with a width of W_s. The coupling between adjacent elements could be adjusted by changing the space between two adjacent elements, basically, the coupling increases with an increasing L_d or W_d for a fixed L or W. When the $50\,\Omega$ lumped feed port was adopted, a simulated 94.8% (from 1.91 to 5.35 GHz) impedance bandwidth (VSWR<2) of the infinite TCPA was observed in [66].
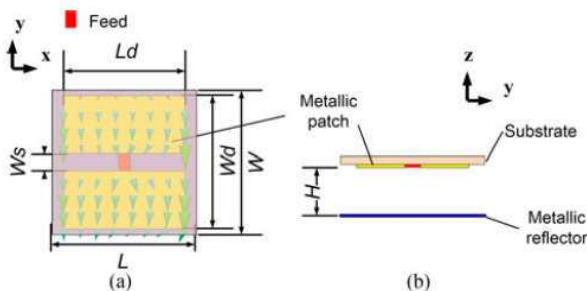

FIGURE 14. **Patch element [66]**

D. FEEDING STRUCTURE

Theoretically, the TCA with ideal feeding exhibit very wide bandwidth, however, the feeding network is bound to be connected to the array element in the practical array, which may cause a dramatic drop of array bandwidth. Therefore, one of the major challenges in realizing a TCA is the design of the array feeding. In most cases, as mentioned above, the array element has a symmetrical structure and when fed with a coaxial cable, a desirable feeding network should have the following properties in entire operating band: 1) transition from the balanced to the unbalanced; 2) impedance transition from 50 Ω (coaxial cable) to the designed input impedance of element; 3) compact size for the low-profile application; 4) common mode resonances mitigation.

In the early TCA design, the elements were fed by a machined device referred as "feed organizer" [4]. A typical feed organizer for a dual-polarization array is not a balun but a grouping of four coaxial cables into a single component, as shown in Fig. 15. The feed organizer provides common-mode suppression and a reliable connection from external components to the TCA elements. However, the feed organizer is a non-planar 3D structure and an external broadband 0-180° hybrid that provides the 180° phase difference between the two coaxial cables driving each arm of a dipole is necessary to each pair of cables.
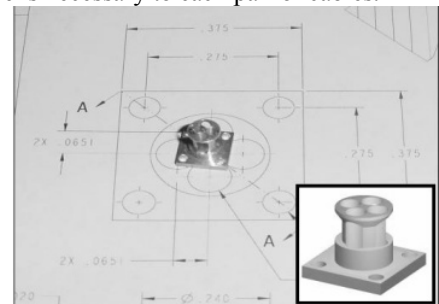
FIGURE 15. **Dual-polarization feed organizer [4]**

The PUMA [28-31] employed a novel feeding scheme which eliminated the need for feed organizer and external hybrid or balun. A cross-sectional view of a PUMA unit cell is depicted in Fig. 16, which shows the unbalanced feed and the shorting vias. As seen, the dipoles are directly fed by a coaxial cable, whose outer conductor is soldered to the ground plane and the center pin is connect to one dipole arm. The other arm is connected to the ground plane through a via. The shorting vias in Fig. 16 can be used to suppress the common-mode resonance without significantly disrupting the desired radiating field. By adjusting the distance from the shoring via to the dipole center, one can shift the common-mode resonance frequency out of the working band. The relationship between the structure parameters and the common-mode resonance frequency could be found in equation (4) in [29]. Although this feed technique is simple, compact and low cost, the bandwidth of the PUMA is only 3:1 or 5:1 with a specially designed matching network.

This article has been accepted for publication in a future issue of this journal, but has not been fully edited. Content may change prior to final publication. Citation information: DOI 10.1109/ACCESS.2018.2873741, IEEE Access

Y. Zhou, F. Zhou, S.Gao etc.: Preparation of Papers for IEEE Access
(September 2018)

FIGURE 16. PUMA feed structure [29]

A small size, X-band wideband feeding balun was proposed in [12] and was presented in previous Fig. 10. The balun is based on a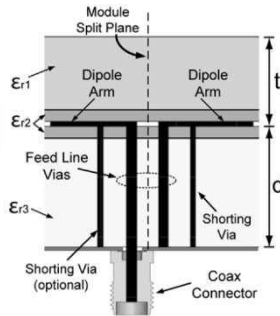 microstrip ring hybrid which employs coupled microstrip lines for bandwidth improvement. The hybrid has two 180° reverse phase output ports extending inside the ring, and a pair of the twin-wire transmission lines are used to connect and match the impedance of the dipole element to the balun impedance. The unit cell width and ground plane spacing is intentionally reduced to shift the common-mode out of the band. However, this feeding balun is not ultra-wideband (8-12.5GHz) and requires a precise fabrication.

In the lower frequency band, if an appropriate ultrawideband balun/impedance transformer was commercially available, the most convenient way to feed was to use off-the-shelf components [11], see Fig. 17. A 10:1 bandwidth was observed.
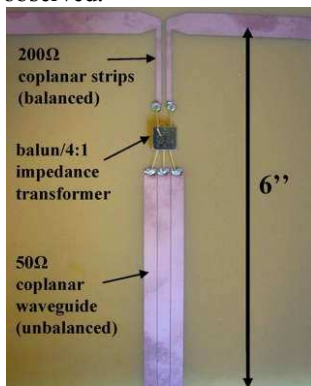

FIGURE 17. Integrated balun [11]

A compact Marchand balun and a wideband impendence matching method based on the Marchand balun were demonstrated in [13]. The basic concept of the wideband impendence matching approach is: the balun may be considered as a part of the impedance matching network for the array element. The reactive of the Marchand balun was employed to cancel that of the element, meanwhile, so-called "double balun" technology was adopted to implement impedance transformation from 50 Ω (coaxial cable) to 200 Ω (dipole element) and to mitigate the common mode resonant. In this way, the overall bandwidth was improved by 30%, compared to the standard feeding techniques. This design approach was named as the TCDA with integrated

balun (TCDA-IB) by authors. TCDA-IB's equivalent circuit model and the implementation of a unit cell are presented as Fig. 18.
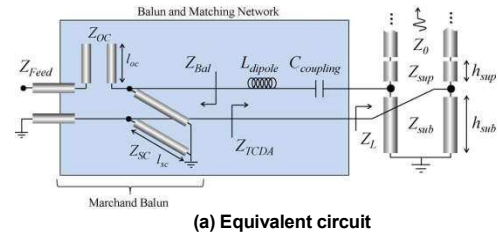
(a) Equivalent circuit
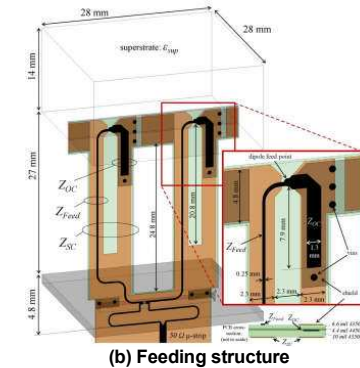
(b) Feeding structure

FIGURE 18. Equivalent circuit and mechanical structure of TCDA-IB [13]

A realistic feed network with a relatively complex structure was proposed in [46], as shown in Fig. 19. The feed included a pair of coplanar stripline (CPS) on the top, the double-Y balun in the middle, and a tapered CPW section at the bottom. Additional vertical and horizontal conductor strips were added from both left and right sides of the balun to prevent common mode resonances. A 1.2-6GHz TCA sample using the feed network was designed, fabricated and measured to verify the validity of the feed structure.
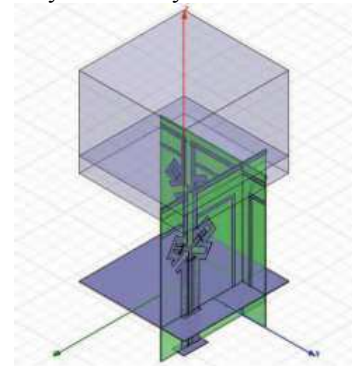
FIGURE 19. Feed structure in [46]

Besides the aforementioned feeding schemes, various baluns were employed in different TCA designs. A coplanar waveguide (CPW) to CPS balun with a radial slot was used in ORA [32], as seen in Fig. 20. A single layer, compact, tapered balun with a >20:1 bandwidth was proposed in [44]. A specially designed S-X band broadband balun which implemented a microstrip to CPS transition and a 1:4 impedance transition was developed in [48].
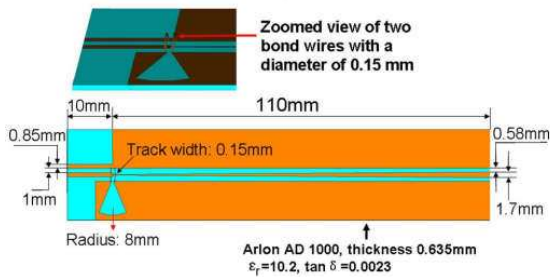
This article has been accepted for publication in a future issue of this journal, but has not been fully edited. Content may change prior to final publication. Citation information: DOI
10.1109/ACCESS.2018.2873741, IEEE Access

IEEE Access

Y. Zhou, F. Zhou, S.Gao etc.: Preparation of Papers for IEEE Access
(September 2018)

FIGURE 20. CPW to CPS Balun in [32]

Thanks to the advances in microwave photonics, optically fed TCA was proposed and developed in [56-58]. The photodiodes were directly integrated with the TCA radiating units, then, each element was driven via an optical fiber instead of a microwave transmission line. The optical feeding scheme circumvents many challenges of the electrical feeding scheme, mainly due to the fact that the ultra-wideband balun is no longer necessary. In addition, the optical feeding scheme can eliminate scan blindness while maintaining broadband, lightweight, and a low profile. Of course, it is understandable that the above advantages are at the expense of the cost, due to the introduction of photodiodes.

The latest progress in the feed technology is the integration of microwave components such as p-i-n diodes, varactors, phase shifters and etc. into the feed network in order to realize a certain level of reconfiguration or multifunction [19, 21, 49 and 59].

E. SUPERSTRATE AND SUBSTRATE

When the concept of TCAs was proposed by Munk, he suggested using dielectric superstrates and magnetic or lossy substrates above the ground plane for further increasing the bandwidth and scan volume of the TCDA.

Initially, the superstrate is one or more layers of dielectric slab placed in front of the array which can mitigate the impedance variation and mismatching when the array beam scan to different angles. This type of supestrate is called wide angle impedance matching (WAIM) layers. Besides the WAIM function, dielectric superstrates can also be used to reduce the characteristic impedance and further improve the array impedance bandwidth [3]. The substrate is usually a lossy material which is introduced to eliminate the "$c/2h$" resonance of an array with ground plane spacing h, thus extending the upper bound of the array working band [3].

A lot of TCA designs utilized the superstrates to improve TCAs performances [7, 12, 13, 14]. Since the dielectric slab WAIM is bulky and heavy, metamaterial or FSS superstrate layers instead of dielectric slabs were applied in some design to reduce the weight and improve the scan volume of TCAs [17, 24, 32, and 53]. In [32], a layer of conductive rings which forms a metamaterial superstrate layer was placed above the array element layer to achieve broader frequency

bandwidth. A novel superstrate consisting of printed frequency selective surface (FSS) for wide angle scanning, as shown in Fig. 21, was used in a TCA design and an impressive 70° scan volume was obtained [17].
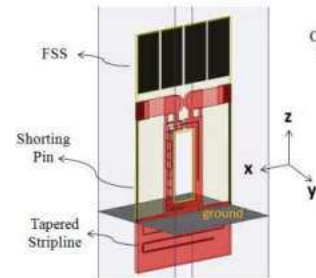
FIGURE 21. FSS superstrate in [17]

Lossy substrates loading technique also is widely used in TCA designs to expand the impedance bandwidth of TCAs at the price of radiation efficiency [7, 14, 18, 48, 52, and 55]. In [7], a ring-type resistive FSS instead of the resistive layer was loaded between the radiating element and ground, the proposed array design achieves a 21:1 bandwidth (infinite array) and greater than 73% radiation efficiency across working frequency band. In [14], the authors employed a resistive substrate loading to enhance array bandwidth and a synergistically designed superstrate to minimize losses from the loading (maintaining radiation efficiency). A bandwidth of 13.9:1 (infinite array, VSWR<2.4) was achieved. In [18] and [48], similar resistive substrate layers were employed following the same principle. In [55], lumped resistors connected in series, as shown in Fig. 22, were used to replace the resistive FSS to reduce the cost and complexity.
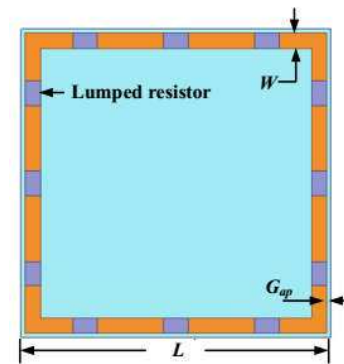
FIGURE 22. FSS substrate using lumped resistors in [55]

F. FINITE ARRAY TECHNOLOGY

Generally, a TCA is initially designed as an infinite array, and a single unit cell is modeled using periodic boundary conditions in an infinite array setting. Although the infinite array approach can provide a computationally efficient analysis, it does not account for edge effects. However, the edge effects in TCAs can be especially severe, due to the edge-born waves, which are generated at the truncated edges of arrays, can propagate almost unattenuated along the arrays. As a result, the impedance of the edge elements of a finite size array usually differs significantly from the intended

9

design. Thus, the edge elements are mismatched and the finite array bandwidth is degraded.

Several techniques have been proposed to alleviate the edge effects. The straightforward way is to terminate edge elements with resistive loads which can absorb the edge-born wave and excite uniformly only at the central portion of the array. However, it will degrade the radiation efficiency [2]. In [62], various edge element termination techniques (resistive, short and open-circuit) were investigated and compared. It was concluded that short-circuit terminations of the peripheral array elements provided a better tradeoff between the impedance bandwidth and efficiency. A TCA using short-circuit terminations of the peripheral array elements was demonstrated in [11], compared with the similar TCA using resistive terminations, an improved efficiency at lower frequencies by a maximum of 47% was achieved. Meanwhile, almost the same bandwidth performance was obtained. Re-designing the edge elements can alleviate the mismatch but at the price of costly computation. In [6], an excitation approach based on characteristic mode theory was proposed to excite a finite TAC that yielded to an increase in both the array efficiency and the realized gain. However non-uniform excitation coefficients and feed line impedances are required which will increase the complexity of the feed system. A novel excitation technique based on reverse scattering for finite-sized beam scanning TCA was proposed in [47], the increased array efficiency and reduced sidelobe levels were preliminarily demonstrated.

G. OTHERS

Besides the above mentioned popular topics, several other interesting subjects on TCAs were studied recently and are reviewed in this section.

Recently, reconfigurable TCAs were studied. In [19, 21], TCAs with tunable rejection bands were proposed by inserting varactor diodes in Marchand balun feed structures. Variable capacitors were used to control the effective length of the balun's short stub to create mismatches at the antenna feed for band rejection. Similarly, a novel way to reconfigure the bandwidth of a TCA was presented in [54]. This was done using a reconfigurable frequency selective surface (FSS) on the top of the array.

Since very small elements and array lattice (comparing to the lower operating wavelength) are used in TCAs, the number of elements and associated T/R modules must be much greater than that of traditional phased arrays which operate in the lower frequency band of TCAs. Therefore, reducing the number of array elements and associated modules while maintaining ultrawideband performances are important for practical applications. The wavelength-scaled array (WSA) architecture was adopted to reduce the element and associated T/R modules of a PUMA by replacing a portion of elements of the periodic array by fewer but scaled up elements that were excited only in lower frequency band

[31], as shown in Fig. 23. A PUMA WSA consisting of a 16×16 6:1 bandwidth PUMA sub-array surrounded by three 8×8 3:1 bandwidth PUMA sub-arrays was analyzed. Numerical results showed that the PUMA WSA had comparable performance to a conventional 6:1 bandwidth PUMA array in terms of the broadside VSWR and gain [31].
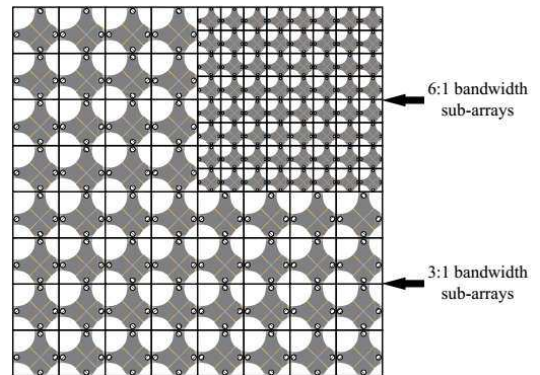
FIGURE 23. PUMA WSA in [31]

The TCA mechanism was also utilized to design antennas with a reduced cut-off frequency and improved bandwidth [63 and 64]. In [63], A wideband horizontally polarized (HP) omnidirectional antenna was proposed, as shown in Fig. 24. It consisted of 12 tightly coupled arc dipole units, 2 rows of parasitic arc strips, a row of director elements and a wideband 1 to 12 feed network. The design in [63] was for a single antenna rather than an antenna array, but the TCA design concepts such as adopting the small element and tight capacitive couple were employed into the design of such an antenna. Owing to the strong mutual coupling and impedance matching layer, the proposed HP omnidirectional antenna has a wide operating band of 70.2% (-10dB return loss).
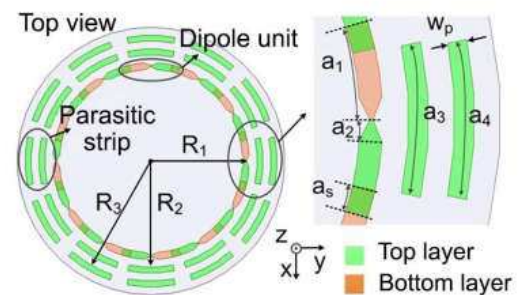
FIGURE 24. Loop antenna with 12 dipoles [63]

The principle of the TCA can also be used to design reflectarray antennas. It is well known that the reflectarray has a simpler feed network than that of conventional array antenna but usually is suffered from a narrow bandwidth. In [69], a novel ultra-wide-band tightly coupled dipole reflectarray (TCDR) was presented. The design in [69] had a wideband reflecting surface which consisted of 26×11 tightly coupled dipole units, as shown in Fig. 25, and they could utilize the combined advantages of reflectarray antennas and those of TCAs. In this way, ultra-wide

This article has been accepted for publication in a future issue of this journal, but has not been fully edited. Content may change prior to final publication. Citation information: DOI
10.1109/ACCESS.2018.2873741, IEEE Access

IEEE Access

Y. Zhou, F. Zhou, S.Gao etc.: Preparation of Papers for IEEE Access
(September 2018)

bandwidth (3.4 to 10.6GHz) was achieved with reduced complexity and manufacture cost. It is the first TCDR design reported.

(a) TCDR element
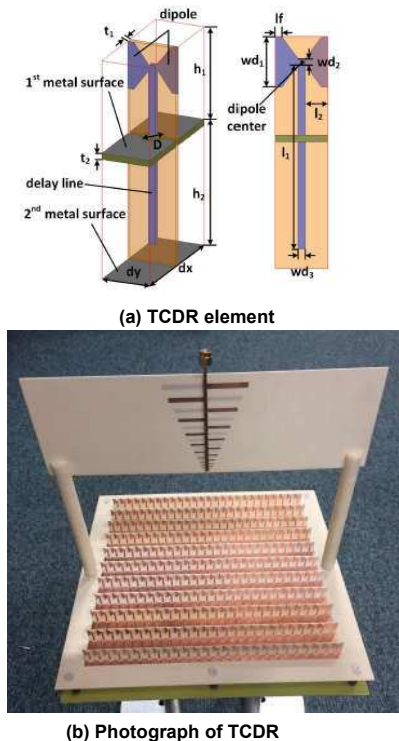
(b) Photograph of TCDR
FIGURE 25. Element and Configure of the TCDR in [69]

Most of the published TCAs are 2D arrays. It is found that 2D TCAs are easier to achieve wideband performances than 1D TCAs. However, wideband linear arrays are needed in several application scenarios. Then, recently 1D TCAs were

studied in [60, 70 and 71]. A dual-polarized 1D TCDA was proposed in [60]. The linear array was designed with the same design principles for 2D TCAD. In order to simulate the 2D working condition, conducting side walls consisting conducting slits and ferrite sheets were placed along the linear array. Another wideband dual-polarized linear array was also introduced in [71]. By strengthening the coupling between the vertical elements which were placed perpendicularly to the array axis and employing a novel vertical superstrate layer, the authors completed a 1D TCA with 4:1 bandwidth, for VSWR<3.0:1, while scanning up to $\pm 60^{\circ}$.

In addition to traditional applications such as communication, radar, and so forth, TCAs have been using in some emerging application areas, for example, RF energy harvesting. A rectifying antenna (rectenna) is needed to harvest RF energy. In [72], a rectenna which has tightly coupled elements was reported. A simulated radiation-to-ac power conversion efficiency of 90% was obtained.

IV TCAS PERFORMANCES

Since the concept of TCAs was presented, many practical TCAs designed by using different techniques and had different improved performances such as bandwidth, scan volume, profile size, etc. were designed. Here, we list some verified typical designs and compare their performances in terms of the bandwidth (BW), the maximum scan angle (θ_{max}), the cross-polarization (C-P), the thickness (T), efficiency (E), and so on, seen in Table 1.

TABLE 1
COMPARISON OF STATE-OF-THE-ART TCAs

Design	BW	θ_{max}	E	C-P	$T(\lambda_h)$	Technical Features
[5]	10:1 (VSWR<2, B. S.*)	N. M.**	N. M.	N. M.	0.55	Spiral element
[7]	21:1 VSWR<3(B. S.)	N. M.	73%	30dB	1.2	Ultra-wideband; Resistive FSS substrate;
[12]	1.6:1 VSWR<2	E-±70° H-±60°	93% (B. S.)	20dB (B. S.) 9.5dB(D-60°)	0.22	Integrated Balun; Shorted Edge Terminations
[13]	7.35:1 VSWR<2.65	±45°	N. M.	20dB	0.76	Integrated Balun
[16]	6:1 VSWR<1.8(B. S.) 2.4(45°), 3.1(60°)	±60°	N. M.	50dB(E/H-60°) 23dB(D-45°), 15dB(D-60°)	0.5	Dual polarizations
[17]	6.1:1 VSWR<3.2	E-±75° D-±70° H-±65°	65% (H-60) 80%	14dB(D-45°) 9dB (D-60°)	0.67	Maximum scan angle; FSS superstrate
[18]	13.5:1 VSWR<2.5(B. S.) 13.1:1	±45°	70%(B. S.) 60%(45°)	20dB	1.1	Ultra-wideband; Substrate loading

	VSWR<3.1(45°)					
[26]	5.23:1 VSWR<3	N. M	N. M	N. M	0.43	Four-square
[29]	5:1 VSWR<2.1(B.S.)	±45°	N. M.	15dB (D-45°)	0.45	PUMA
[30]	3:1 VSWR<2.1(B.S.) 2.8	±45°	N. M.	15dB (D-45°)	0.43	PUMA
[32]	3.3:1 VSWR<3	±45°	N. M.	15dB (D-45°)	0.5	Octagonal Ring Element
[48]	5:1 VSWR<2 (B.S.), 2.5	±45°	N. M.	15dB	0.2	
[51]	2.5:1 VSWR<2	±60°	N. M.	19dB (B. S.) 13dB (75°)	0.44	Wide angle steering; parasitic ring loading

* B. S.: Broadside Scan

** N. M.: No Mention

V CASE STUDY

A Low-profile wideband wide-scan tightly coupled array antenna is developed as a design example.

A. ANTENNA DEVELOPMENT

In this case study, the development of a tightly coupled array antenna featuring the characteristics of wideband, wide-scan and low-profile is described. The main specifications of the antenna include:
1) Bandwidth: 3:1
2) Scan range: ±45°
3) Thickness: $\leq \lambda_h/2$, λ_h is the wavelength at the highest operating frequency in free space.

In practice, the challenges of achieving the tightly coupled array antenna include the feeding and the impedance matching over wide scan angles. Ideally, wideband baluns are suitable for exciting the balanced dipoles while it leads to much complexity, cost, volume, and loss. An alternative method is to employ the simplified unbalanced feeding, while the problematic common-mode resonance leads to null radiation at boresight. The relationship between the resonant frequency and the structure of the element has been explicitly explained in [65]. Consequently, a suppression scheme needs to be developed when unbalanced exciting balanced dipole arms. On the other hand, it is difficult to match the high impedance ($\approx 377\Omega$) to 50Ω via the unbalanced feeds especially scanning up to large angles.

To address the above-mentioned challenges, a novel method has been proposed to overcome the common-mode resonance when unbalanced structure feeding the balanced dipoles. As shown in Fig. 26, the presented antenna has three layers of Duroid 5880 substrates with a dielectric constant of 2.2 and thicknesses of h_1, h_2 and h_3, respectively. The dipole arms are printed on the top side of the middle layer. A simple unbalanced feeding mechanism is employed to feed the antenna with the left feeding via connected to the 50Ω connector and the right one attached to the ground plane. Be

noted that a loaded cross-shaped patch on the back side of the middle substrate is used to avoid the common-mode resonance over the operating frequency band. It is directly connected to the ground plane through several conducting vias. The top layer substrate is utilized to achieve good impedance matching when scanning up to large angles. It can also be observed as a radome to protect the antenna. The phased antenna array is arranged in a rectangular lattice with a size of D_x by D_y (7mm × 7mm). Thus, the highest operating frequency of avoiding the grating lobe is around 21GHz. The whole thickness of the antenna structure is 4.5mm corresponding to $0.32\lambda_h$.
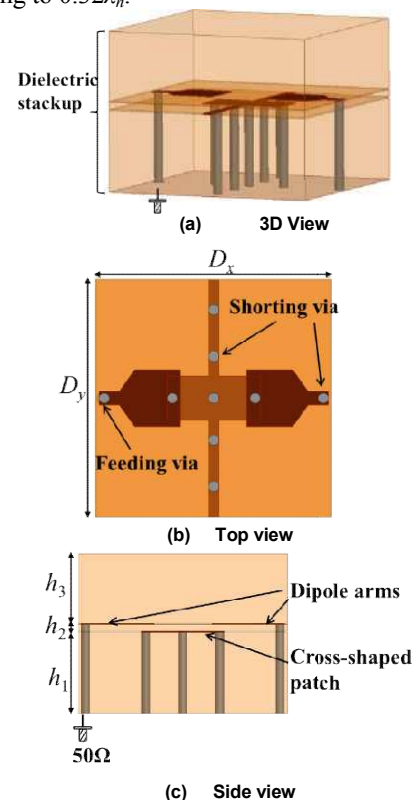

(a)   3D View

(b)   Top view

(c)   Side view

FIGURE 26. The structure and geometry of the tightly coupled phased array antenna.

B. Results and Discussions

To quickly obtain the overall performance of the proposed array element, the infinite array, unit-cell simulations have been carried out using Ansoft's HFSS. A PML absorber terminates the top of the model and is separated around $\lambda_l/2$ from the top of the element. Periodic boundary conditions (PBC) are applied on the four sides of the model and provide an infinitely periodic dimension. Fig. 27 presents the simulated scan VSWR results in both E- and H-planes. As observed, the results suggest VSWR ≤ 2 at broadside over 6.9-21.8 GHz, indicating that the common-mode resonance frequency is above the grating lobe frequency. The VSWR in the E-plane remains constant and is below 2.2 over various scan angles though the highest frequency is moved downward. It is also noted that the VSWR in the H-plane is less than 2.5 when scanned to θ = 45°.

The infinite array with unit-cell model was employed to obtain the embedded element patterns at various frequencies, as shown in Fig. 28. Compared with finite size simulation model, it took less time and avoided the edge truncation error. As observed, the array achieves symmetrical patterns in both principal planes. The gain variation versus scanning angles is less than 2.2 dB in both planes, indicating good radiation performance over wide scan range. The cross-polarization level is less than -50 dB in the E-plane at each frequency, while the cross-polarization level changes versus frequency in the H-plane. It is also noticed that the cross-polarization level in the H-plane increases when scanning up to large angles and becomes null at boresight. The characteristics of cross-polarized radiation patterns of the presented tightly coupled array antenna are similar to the typical microstrip antennas.

Fig. 29 presents the simulated boresight realized gain in the unit-cell model compared with the ideal gain ($4\pi A/\lambda^2$), where A is the aperture area of the unit-cell and λ corresponds to free space wavelength. The maximum difference between the two curves is less than 0.6 dB in the lower band. The radiation efficiency and return loss account for the loss.

In order to obtain measurement data of the TCA, finite array simulations and optimizations should be carried out using HFSS or other simulation tools. For the broadside measurements, a wideband power divider can be connected to the array, to achieve uniform excitation. According to references [14, 16, 17, 18 etc.], the measured scanned patterns for a finite array can be obtained using the unit-excitation active element pattern method. For simplicity, the simulation and measurement results for the finite array are not provided here.

a) E-plane
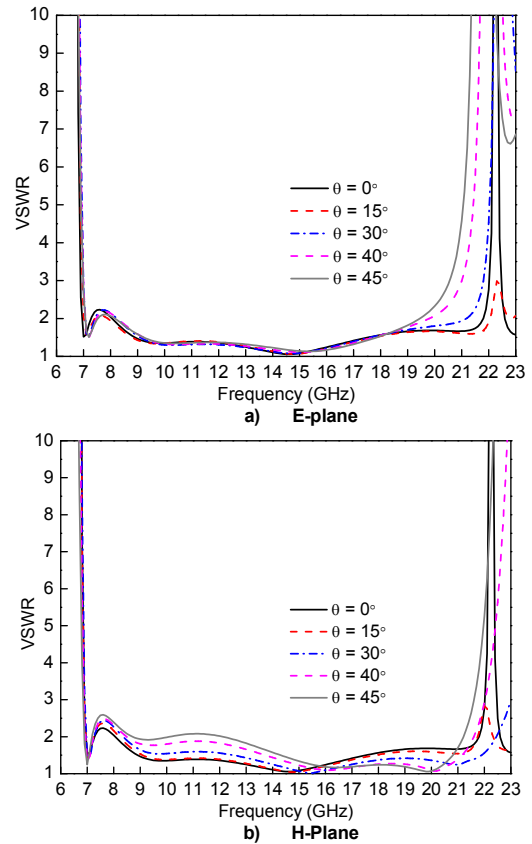
b) H-Plane

FIGURE 27. VSWR versus frequency and scan angle of the infinite array.
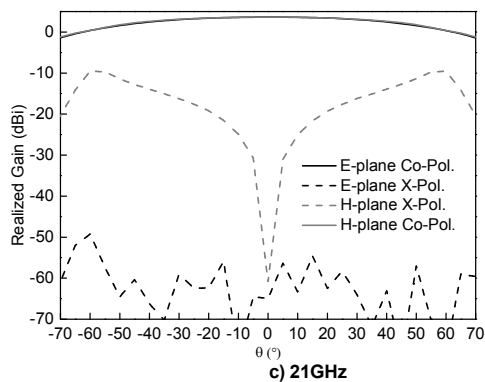

a) 7GHz

b) 13GHz
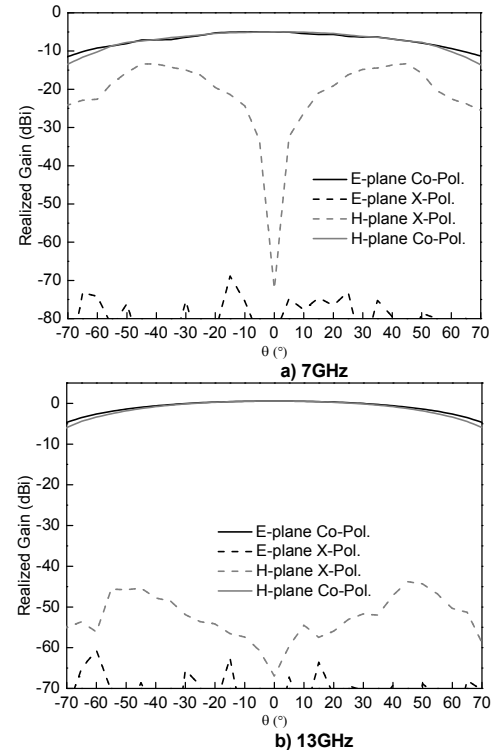
FIGURE 28. Simulated central element patterns in both E- and H-planes at various frequencies.
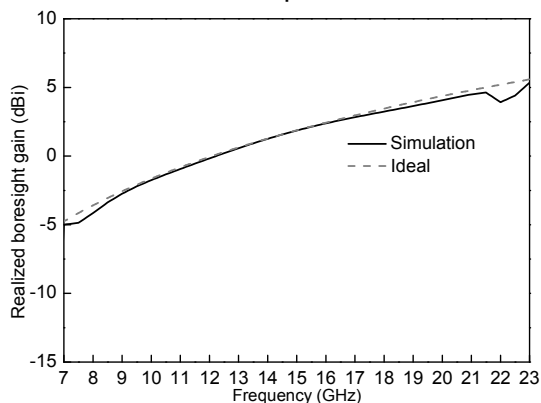

FIGURE 29. The simulated boresight absolute gain in the unit-cell model compared with ideal gain.

VI CONCLUSION AND FUTURE TREND

In this paper, we discussed recent development of the TCAs which utilize the capacitive coupling. The operation principle and the evolution of the TCAs were reviewed at first. Then, a review of recent development in the analysis and design of TCAs, such as equivalent circuit analysis, bandwidth limits analysis, array elements, feed structures, substrates/superstrates loading, etc., were illustrated in details and the performances of state-of-the-art TCAs were provided and compared. Finally, one case study showing the detailed step-by-step process of TCA design was given to show the TCA's theory, principle and design methodology..

After more than one decade of development, many types of TCAs with wideband performance have been designed, fabricated and measured. Very excellent performances, such as bandwidth (up to 67:1), scan volume (up to 75°) and thickness (less than $0.05\lambda_l$) have been reported. The future development of TCAs will focus on several aspects: 1). The reduction of the size, complexity and cost of TCA; 2). Further improvement of radiation performance in terms of frequency range, beam scanning range, antenna gain, efficiency, etc; 3). System implementation using a combination of TCA with the beamforming networks such as optically feed networks or digital beamforming sub-systems. Since an array lattice of one-half wavelength of the highest working frequency is usually adopted in TCAs, in the lower

operating frequency band, compared with traditional phased arrays with the same electrical size, the TCAs employ more elements and associated T/R modules, then the complexity and cost of arrays are increased. The technology of reducing the scale of feeding system, thus decreasing the cost and complexity of TCAs is one of the research topics worth to be investigated. The TCAs have achieved excellent performances. It is very difficult to further improve their performances with traditional methods. The reconfigurable structure can be used to further improve TCAs' performances or develop additional functions. For example, in order to suppress interference, tunable rejection band of the TCA can be dynamically introduced. The coupling between elements can be real-time adjusted to adapting different scan conditions and so on. Reconfigurable TCA will be the future development of the TCA technology. The radiation aperture of the TCA has the ultra-wide bandwidth, but the associated feed network is usually difficult to implement with the same bandwidth. The feed network may be the bandwidth bottleneck of the whole array. It is logical to integrate the broadband TCA aperture and broad optical feed network. The optically-fed TCA is a promising technology. It is expected that TCAs will find more practical applications in the near future.

REFERENCES

[1]   H. Wheeler, "Simple relations derived from a phased-array antenna made of an infinite current sheet," *IEEE Trans. Antennas Propag.*, vol. 14, no. 4, pp. 506-514, 1965.

[2]   B. Munk, R. Taylor, W. Croswell, B. Pigon, R. Boozer, S. Brown, M. Jones, S. Pryor, S. Ortiz, J. Rawnick, K. Krebs, M. Vanstrum, G. Gothard, and D. Wiebelt, "A low profile broad band phased array antenna," in Proc. AP-S Symp., Columbus, OH, 2003, pp. 448–451.

[3]   B. Munk, "Finite Antenna Arrays and FSS," Piscataway/Hoboken, NJ, USA: IEEE Press/Wiley-Interscience, 2003 , ch. 6, pp. 181–213.

[4]   M. Jones and J. Rawnick, "A new approach to broadband array design using tightly coupled elements," in Proc. IEEE MILCOM, 2007, pp. 1–7.

[5]   I. Tzanidis, K. Sertel, and J. L. Volakis, "Interwoven spiral array (ISPA) with a 10:1 bandwidth on a ground plane," *IEEE Antennas Wireless Propag. Lett.,* vol. 10, no. 3, pp. 115–118, Mar. 2011.

[6]   I. Tzanidis, K. Sertel, and J. L. Volakis. "Characteristic Excitation Taper for Ultrawideband tightly coupled antenna arrays," *IEEE Trans. Antennas Propag.*, vol. 60, no. 4, pp: 1777-1784 Apr. 2012.

[7]   W. F. Moulder, K. Sertel, and J. L. Volakis, "Superstrate-enhanced ultrawideband tightly coupled array with resistive FSS," *IEEE Trans. Antennas Propag.*, vol. 60, no. 9, pp: 4166-4172, Sep. 2012.

[8]   J. P. Doane, K. Sertel, and J. L. Volakis, "Bandwidth limits for lossless planar arrays over ground plane," Electron. Lett., vol. 48, no. 10, pp. 540–542, 2012.

[9]   E. A. Alwan, K. Sertel, and J. L. Volakis, "A simple equivalent circuit model for ultrawideband coupled arrays," *IEEE Antennas Wireless Propag. Lett.,* 2012, vol. 11, pp. 117–120.

This article has been accepted for publication in a future issue of this journal, but has not been fully edited. Content may change prior to final publication. Citation information: DOI
10.1109/ACCESS.2018.2873741, IEEE Access

IEEE Access

Y. Zhou, F. Zhou, S.Gao etc.: Preparation of Papers for IEEE Access
(September 2018)

[10] J.P. Doane , K. Sertel, J. L. Volakis,"Matching bandwidth limits for arrays backed by a conducting ground plane," *IEEE Trans. Antennas Propag.*, vol. 61, no. 5, pp. 2511-2518, May 2013.

[11] I. Tzanidis, K. Sertel, and John L. Volakis. "UWB low-profile tightly coupled dipole array with integrated balun and edge terminations," *IEEE Trans. Antennas Propag.*, vol. 61, no. 6, pp. 3017-3025, Jun. 2013.

[12] J. A. Kasemodel, C. Chen, and J. L. Volakis, "wideband planar array with integrated feed and matching network for wide-angle scanning," *IEEE Trans. Antennas Propag.*, vol. 61, no. 9, pp. 4528-4537, Sep. 2013.

[13] J. P. Doane, K. Sertel, and J. L. Volakis, "A wideband wide scanning tightly coupled dipole array with integrated balun (TCDA-IB)," *IEEE Trans. Antennas Propag.*, vol. 61, no. 9, pp. 4538-4548, Sep. 2013

[14] W. F. Moulder, K. Sertel, and J. L. Volakis, "Ultrawideband Superstrate-Enhanced Substrate-Loaded array with integrated feed," *IEEE Trans. Antennas Propag.*, vol. 61, no. 11, pp. 5802-5807, Nov. 2013

[15] J. P. Doane , K. Sertel, and J. L. Volakis, "Bandwidth Limits for Lossless, Reciprocal PEC-backed arrays of arbitray polarization," *IEEE Trans. Antennas Propag.*, vol. 62, no. 5, pp. 2531-2541, May 2014.

[16] Ma. H. Novak, and J. L. Volakis, "Ultrawideband antennas for multiband satellite communications at UHF-Ku Frequencies," *IEEE Trans. Antennas Propag.*, vol. 63, no. 4, 1334-1341, Apr. 2015.

[17] E. Yetisir, N. Ghalichechian, and J. L. Volakis, "Ultrawideband array with 70° scanning using fss superstrate," *IEEE Trans. Antennas Propag.*, vol. 64, no. 10, pp.4256-4265, Oct. 2016.

[18] D. K. Papantonis, and J. L. Volakis, "Dual-polarized tightly coupled array with substrate loading," *IEEE Antennas Wireless Propag. Lett.,* vol. 15, pp. 325-328, 2016.

[19] D. K. Papantonis, E. Yetisir, N. Ghalichechian, and J. L. Volakis, "Tunable Band Rejection In A Tightly-Coupled Array using varactor diodes," *in Proc. iWAT,* Feb.29-Mar. 2 2016, pp. 20-22.

[20] M. H. Novak, F. A. Miranda, and J. L. Volakis, "An Ultra-Wideband Millimeter-Wave Phased array", *in Proc. EuCAP,* Apr. 10-15, 2016, pp.1-3

[21] D. K. Papantonis, E. Yetisir, N. Ghalichechian, and J. L. Volakis," Tunable Band Rejection of Wideband Arrays Using Digital variable capactiors," *in Proc. APSURSI,* Jun.26-Jul.1, 2016, pp.647-648.

[22] S. B. Venkatakrishnan, A. Akhiyat, E. A. Alwan, and J. L. Volakis, "multi-band and multi-beam direction of arrival estimation using on-site coding digital beamformer," *IEEE Antennas Wireless Propag. Lett.,* vol. 16, pp. 2332-2335, Jun. 2017.

[23] C. W. Lee, D. Papantonis, A. Kiourti and J. L. Volakis, "Body-Worn 67:1 Bandwidth Antenna Using 3 overlapping dipole elements," *in Proc. EuCAP,* Mar. 19-24, 2017, pp. 1557-1558.

[24] J. Zhong, E. A. Alwan and J. L. Volakis, "Ultra-Wideband Dual-Linear Polarized Phased Array with 60 scanning for simultaneous transmit and receive systems," *in Proc. iWAT,* Mar. 1-3, 2017, pp.140-141.

[25] T. R. Vogler and W. Davis, "Analysis and modification of the infinite foursquare array," *in Proc. APSURSI*, Jul. 2010, pp. 1-4.

[26] T. R. Vogler, "Analysis of the Radiation Mechanisms in and Design of Tightly-Coupled Antenna Arrays," Ph.D. dissertation, Virginia Tech, 2010.

[27] J. R. Nealy, "Foursquare antenna radiating element." U.S. Patent 5 926 137, Jul. 20, 1999.

[28] S. S. Holland and M. N. Vouvakis, "A 7–21 GHz planar ultrawideband modular antenna array," *in Proc. APSURSI,* Jul. 11-17, 2010, pp. 1-4.

[29] S. S. Holland and M. N. Vouvakis, "The planar ultrawideband modular antenna (PUMA) array," *IEEE Trans. Antennas Propag.,* vol. 60, no. 1, pp. 130–140, Jan. 2012.

[30] S. S. Holland and M. N. Vouvakis, "A 7-21GHz Dual-Polarized Planar Ultrawideband Modular Antenna (PUMA) Array," *IEEE Trans. Antennas Propag.,* vol. 60, no. 10, pp. 4589–4600, Oct. 2012.

[31] M. Y. Lee, R. W. Kindt and M. N. Vouvakis. "Planar Ultrawideband modular antenna wavelength-scaled array," *in Proc. APSURSI,* Jun.26-Jul.1, 2016, pp.345-346.

[32] Y. Zhang and A. K. Brown, "Octagonal Ring Antenna for a Compact Dual-Polarized Aperture array," *IEEE Trans. Antennas Propag.,* vol. 59, no. 10, p.3927-3932, Oct. 2011

[33] E. Farhat, K. Adami, Y. Zhang, A. Brown,and C. Sammut, "Ultra-wideband tightly coupled fractal octagonal phased array antenna," *in Proc. ICEAA,* Sept 2013, pp. 140–144.

[34] E. O. Farhat, K. Z. Adami, Y. Zhang, A. K. Brown, C. V. Sammut, and J. Abela, "Aperture Arrays for Radio Astronomy," *in Proc. ICEAA,* Aug. 3-8, 2014, pp.185-190.

[35] I. O. Farhat1, K. Z. Adami1, J. Abela1, and C. V. Sammut, "Genetic Algorithm Application on a Tightly Coupled array antenna," *in Proc. EuCAP,* Mar. 19-24, 2017, pp.2281-2285.

[36] B. Riviere, H. Jeuland, and S. Bolioli, "new equivalent circuit model for a broadband optimization of dipole arrays," *IEEE Antennas Wireless Propag. Lett.,* vol. 13, pp. 1300-1304, 2014.

[37] D. Cavallo, W. H. Syed and A. Neto, "Equivlent transmission line models for the analysis of edge effects in finite connected and tightly coupled arrays," *IEEE Trans. Antennas Propag.*, vol. 65, no. 4, pp.1788-1796, Apr. 2017.

[38] H. Chang and D. Kwon, "Higher-Order Bandwidth Bounds for conductor-backed planar arrays," *in Proc. APSURSI*, Jun.26-Jul.1, 2016, pp.921-922.

[39] H. Lee, S. Nam, "A 3.37 vs 1 Bandwidth and Low-profile Tightly coupled array antenna," *in Proc. ISAP*, Oct. 24-28, 2016, pp.404-405.

[40] S. Lu, C. Gu, G. Han, Z. Zhou, X. Li, and Z. Li, "A Double Dipoles per Cell Structure for Solving common-mode resonance in tightly coupled dipole array," *in Proc. ICMMT*, Jun. 5-8, 2016, pp. 829-831.

[41] J. Dai, H. Wang, H. Wang, X. Jiang, D. Xu, and Y. Huang, "A Low-profile, Decade Bandwidth tightly-coupled vivaldi phased array," *in Proc. ISAP*, Oct. 24-28, 2016, pp.688-689.

[42] Y. Wang , F. Zhu , and S. Gao, "Design of a Low-profile 2-10 GHz Ultra-wideband Antenna Array," *in Proc. PIERS*, Aug. 8-11, 2016, pp.2041-2043

[43] Y. Wang, S. Qu, and S. Yang, "Ultra-Wideband Wide-Scan Tightly Coupled Dipole array," *in Proc. iWEM*, May 30 - Jun. 1, 2017, pp.171-172.

This article has been accepted for publication in a future issue of this journal, but has not been fully edited. Content may change prior to final publication. Citation information: DOI 10.1109/ACCESS.2018.2873741, IEEE Access

IEEE Access

Y. Zhou, F. Zhou, S.Gao etc.: Preparation of Papers for IEEE Access
(September 2018)

[44] A. O. Bah, P. Qin, and Y. Jay Guo, "An Extremely Wideband Tapered Balun for Application in Tightly coupled array," *in Proc. APMC*, Sep. 19-23, 2016, pp. 162-165.

[45] M. H. Novak, F. A. Miranda and J. L. Volakis, "An Ultra-Wideband Millimeter-Wave Phased array", *in Proc. EuCAP*, Apr. 10-15, 2016, pp.1-3.

[46] A. Boryssenko, T. Goodwin, "Broadband Antenna Array Aperture Made of Tightly coupled printed dipoles," *in Proc. PAST*, Oct. 18-21, 2016, pp. 1-6.

[47] A. A. Salih, and Z. N. Chen, "Excitation for Tightly Coupled Beam Scanning Antenna Array Based on inverse scattering," *in Proc. NEMO*, Jul. 27-29, 2016.

[48] H. Huang, K. Xiao, L. Ding, S. Wang and S. Chai, "Ultrawideband Tightly Coupled Array For multiband communications at S-X frequencies," *in Proc. iWEM*, May 16-18, 2016.

[49] A. J. Abumunshar, N. K. Nahar1, and K. Sertel. "18-40GHz Low-profile Phased Array with Integrated MEMS phase shifters," *in Proc. EuCAP*, Mar. 19-24, 2016

[50] X. Li, C. Gu, G. Han, Z. Zhou, S. Lu, and Zhuo Li, "A UWB Wide-scan Tightly Coupled Dipole Array," *in Proc. iWEM,* May 16-18, 2016, pp.1-3.

[51] H. H. Vo, C. Chen, P. Hagan, and Y. Bayram, "A Very Low-Profile UWB Phased Array Antenna desigh for supporting wide angle beam steering," *in Proc. PAST,* Oct. 18-21, 2016, pp.1-8.

[52] L. zhou, S. Yang, Z. Guo, and Y. Chen, "A Wideband Dual-Polarized Dipole Linear Array with resistive loading," *in Proc. IMWS-AMP*, Jul. 20-22, 2016, pp.1-3

[53] X. Yang, G. Zhao, W. Hu, Y. Jay Guo, Y. Z. Yin and A. O. Bah, "Characteristics of Wideband Phased Array with Two-layer metasurface," *in Proc. ICEAA*, Sept. 18-23, 2016, pp. 852-855

[54] D. K. Papantonis, E. Yetisir, and J. L. Volakis, "Tightly-coupled Array with Tunable BW using reconfigurable FSS superstrate," *in Proc. USNC-URSI*, Jun.26-Jul.1, 2016, pp.13-14

[55] W. Zou, S. Qu, Y. Chen, and S. Yang, "A Planar Ultrawideband Linear Array with resistor-loaded FSS," *in Proc. iWEM*, May 30 – Jun. 1, 2017, pp.126-127.

[56] S. Shi, J. Bai,, R. Nelson, C. Schuetz, *et al.*, "Ultrawideband optically fed tightly coupled phased array," *J. of Lightwave Technol.*, vol. 33, no. 23, pp.4781-4790, Dec. 2015

[57] M. R. Konkol, D. D. Ross, S. Shi, *et al.*, "High-power photodiode-integrated-connected array antenna," *J. of Lightwave Technol.*, vol. 35, no. 10, pp. 2010-2016, May 15, 2017.

[58] D. D. Ross, M. R. Konkol, S. Shi, *et al.*, "Low-profile High power optically addressed phased array antenna," *J. of Lightwave Technol.*, vol. 35, no. 18 pp. 3894-3900, 2017.

[59] A. J. Abumunshar, N. K. Nahar1, and K. Sertel. "K-to-Ka Band Low-profile Phased Array with Integrated MEMS Phase Shifters," *in Proc. APSURSI*, Jun.26-Jul.1, 2016, pp.1143-1144.

[60] H. Lee, and S. Nam, "a dual-polarized 1D tightly coupled dipole array antenna," *IEEE Trans. Antennas Propag.*, vol. 65, no. 9, pp. 4511-4518, Sept. 2017.

[61] A. Boryssenko and T. Goodwin, "Broadband Antenna Array Aperture Made of Tightly coupled printed dipoles," *in Proc. PAST*, Oct. 18-21, 2016, pp. 1-6.

[62] I. Tzanidis, K. Sertel, and J. Volakis, "Excitation and termination of finite tightly coupled antenna arrays based on structural characteristic modes," *in Proc. Antenna Applications Symp.,* Sep. 2011.

[63] Z. D. Wang, Y. Z. Yin, X. Yang, and J. J. Wu, "design of a wideband horizontally polarized omnidirectional antenna with mutual coupling method," *IEEE Trans. Antennas Propag.*, vol. 63, no. 7, pp. 3311-3316, Jul. 2015.

[64] H. Liu, Y. Liu, W. Zhang, and S. Gao, "an ultra-wideband horizontally polarized omnidirectional circular connected vivaldi antenna array," *IEEE Trans. Antennas Propag.*, 2017, vol. 65, no. 8, pp. 4351-4356, Aug. 2017.

[65] S. S. Holland, "Low-*profile, M*odular, Ultra-Wideband Phased Arrays," Ph.D. dissertation, Dept. Elect. & Comp. Eng., Univ. of Massa., Amherst, MA, USA, 2011.

[66] X. Yang *et al.* "Analysis and Design of a Broadband Multifeed Tightly Coupled Patch Array Antenna," *IEEE Antennas Wireless Propag. Lett.,* vol. 17,.no. 2, pp. 217-220, Feb. 2018.

[67] E. Irci, K. Sertel, and J. L. Volakis, "An extremely low profile, compact, and broadband tightly coupled patch array," *Radio Sci.,* vol. 47, no. 3, pp. 1–13, Jun. 2012.

[68] M. R. Konkol, D. D. Ross, S. Shi *et al.* "Photonic Tightly Coupled Array," *IEEE Trans. Microw. Theory Techn.*, vol. 66, no. 5, pp. 2570-2578, May 2018.

[69] W. Li, S. Gao, L. Zhang *et al.* "An Ultra-Wide-Band Tightly Coupled Dipole Reflectarray Antenna," *IEEE Trans. Antennas Propag,* vol. 66, no. 2, pp. 533-540, May 2018.

[70] Y. Wang, L. Zhu, H. Wang *et al.* "A Compact, Scanning Tightly Coupled Dipole Array With Parasitic Strips for Next-Generation Wireless Applications," *IEEE Antennas Wireless Propag. Lett.,* vol. 17, no. 4, pp. 534-537, Apr. 2018.

[71] T. S. Almoneef, F. Erkmen, M. A. Alotaibi *et al.* "A New Approach To Microwave Rectennas Using Tightly Coupled Antennas," *IEEE Trans. Antennas Propag,* vol. 66, no. 4, pp. 1714-1724, Apr. 2018.

[72] H. Zhang, S. Yang, Y. Chen *et al.* "Wideband Dual-Polarized Linear Array of Tightly Coupled Elements," *IEEE Trans. Antennas Propag,* vol. 66, no. 1, pp. 476-480, Jan. 2018.